Single-Stranded Breaks Relax Intrinsic Curvature in DNA?

Dimitri E. Kamashev[§] and Alexey K. Mazur*

CNRS UPR9080, Institut de Biologie Physico-Chimique, 13 rue Pierre et Marie Curie, Paris 75005, France

Received December 17, 2003; Revised Manuscript Received April 23, 2004

ABSTRACT: The recent hypothesis of a compressed backbone state as the origin of the intrinsic curvature in DNA suggested that it could result from a geometric mismatch between the partial specific backbone length and optimal base stacking. It predicted that the long-known phenomenon of static curvature in A-tract repeats may be affected by single-stranded breaks (nicks) that should relax it in a position-dependent manner. To check the aforementioned prediction, a special series of nicked DNA fragments was prepared from two mother sequences, one including phased A-tract repeats and the other being random, and the curvature was probed experimentally by gel mobility assays. In agreement with earlier reports, single-stranded breaks produce virtually no effect upon the gel mobility of the random sequence DNA. In contrast, for nicked A-tract fragments, the curvature exhibits regular periodical behavior depending upon the position of the strand break with respect to the overall bend. The modulations are rather strong, with the maximal increase in gel mobility exceeding 30% of the initial difference with respect to the reference straight DNA. This effect has not been encountered before, and it is opposite the usual nonspecific retardation caused by single-stranded breaks. The amplitude of the observed modulation is increased for phosphorylated nicks and in the presence of Mg^{2+} ions.

The intrinsic curvature in DNA was discovered about 20 years ago for regular repeats of A_nT_m, with $n + m > 3$, called A-tracts (*1*−*4*), and also for other sequences some years later (*5*, *6*). Several profound reviews exist of the large volume of related data accumulated during the past couple decades (*7*−*12*). The exact physical origin of this phenomenon remains unclear. Because of that and due to its outstanding role in genome functioning, it continues to attract great attention (*13*−*19*). A number of its possible mechanisms were proposed in the literature, and we will briefly review the most important of them in the Discussion and Conclusions. Although none of these mechanisms were able to resolve all the controversies, some models gained partial support from experiments suggesting that they correctly describe certain features of the real situation. It is possible also that more than one distinct factor is responsible for this effect and that the mechanisms now considered as alternative in fact act concertedly. However, a coherent unified picture is not yet available.

Yet another hypothesis of the origin of intrinsic curvature has been recently proposed on the basis of the results of free molecular dynamics simulations of A-tract repeats (*20*−*22*). It postulates that bends in a double helix can be caused by stipulated inherent compression of the sugar−phosphate backbone in B-DNA that results from a geometric mismatch between its intrinsic length and that dictated by the base pair stacking. Starting from the first published drawing of the double helix (*23*), its two backbone strands are viewed as regular spiral traces that wind along the surface of the cylindrical B-DNA core formed by stacked base pairs. Because regular spirals represent the shortest lines that join two points on a cylindrical surface, and because the backbone strands are covalently linked to bases, an ideal B-DNA can exist only if the average backbone length either matches exactly or is shorter than that dictated by the base pair stacking (*21*). The compressed backbone hypothesis (CBH)[1] assumes the opposite. It postulates that, under physiological conditions, the equilibrium specific length of the B-DNA backbone, considered as a restrained polymer attached to a cylindrical surface, is slightly longer than in the canonical B-form. In physics, a similar mismatching relationship is often called geometric frustration (*24*). The backbone tries to expand and "pushes" stacked bases while the stacking interactions oppose this. Eventually, the backbone finds a "compromise" by deviating from its regular spiral trace, which causes quasi-sinusoidal modulations of the DNA grooves. Concomitant base stacking perturbations cause local bends that accumulate to macroscopic static curvature when the period of these modulations corresponds to an integral number of helical turns. The possibility of such a mechanism can be illustrated by the following simple argument. Consider a straight double helix subjected to a weak unwinding torsional stress. Under a certain degree of unwinding, a bending deformation emerges, which is well described by the elastic rod DNA model and supported by experimental data. According to CBH, the intrinsic curvature emerges in essentially the same way, with a distributed torsional stress produced by the core of the double helix due to the aforementioned geometric mismatch. A detailed discussion of CBH and its consequences can be found in our previous papers (*20*−*22*).

[§] Current address. CNRS UPR9051, Hôpital St. Lois, 1 av. C. Vellefaux, 75475 Paris Cedex 10, France.

[1] Abbreviations: CBH, compressed backbone hypothesis; MD, molecular dynamics; PAGE, polyacrylamide gel electrophoresis; EDTA, ethylenediaminetetraacetic acid.

10.1021/bi036266a CCC: $27.50
Published on Web 06/03/2004

The above hypothesis continues the line of earlier mechanisms that attributed the origin of bending to the properties of the DNA backbone (*25*−*27*). If it proved true, this would change significantly our view of the fundamental properties of duplex DNA and especially its slow dynamics because the microscopic mismatching relationship can result in macroscopic relaxation times. This model offers new interpretations to long-standing unclear observations in this field, and it is the only one that agrees with the nature of static bends obtained in free MD simulations (*20*−*22*). For a stringent verification, however, one should find and test experimentally some new and nontrivial theoretical predictions. Two such possibilities have been proposed (*20*), and the first and more simple of them is the subject of the present study.

According to CBH, the intrinsic curvature in DNA can be relaxed by introducing single-stranded chain breaks (nicks) (*20*). Reversible nicks as well as single-stranded gaps in DNA occur during diverse biochemical processes, including general and site-specific recombination, replication, and DNA repair. The corresponding structural perturbations have been previously characterized in a number of experimental studies (*28*−*44*). According to all these data, nicks perturb the free DNA very little. The corresponding X-ray structures (*34*) are straight and similar to those of intact duplexes with analogous sequences. This agrees with early physicochemical tests (*28*−*30*) as well as NMR studies in solution (*32*, *33*, *41*−*43*). The main detectable effect of a nick is local melting or fraying, especially at low ionic strength, mild denaturating conditions, or elevated temperatures. This increases the isotropic flexibility of DNA and reduces its gel mobility (*36*, *37*, *39*, *44*). In normal conditions the nick fraying is small, and it is almost undetectable below 10 °C (*37*, *44*).

On the basis of these experimental data and the earlier views of the origin of intrinsic curvature, one should expect that nicks in phased A-tract sequences can either increase bending or have zero effect. The increase may be expected if the curvature is caused by external forces, as in electrostatic counterion models, because the flexible hinge at a nick can allow these forces to increase the bend angle in their direction. A zero effect is expected for the wedge and junction models because nicks arguably do not affect the A-tract structures (*34*) and do not cause wedges detectable in gel migration assays (*37*). In contrast, if the intrinsic curvature is really caused by the backbone compression, single-stranded breaks should relax the compression, which should increase the gel mobility of curved DNA fragments. This effect is opposite that of the increased isotropic flexibility; moreover, the latter can be eliminated by reducing the temperature so that these two phenomena cannot be confused. In addition, because the degree of the compression should vary regularly between the inner and outer edges of the bent DNA, relaxation produced by a single nick is expected to change systematically according to its position with respect to the overall bend.

Here we present the results of an experimental study carried out according to the above plan. Two 35-mer sequences were used for constructing several series of nicked DNA fragments. The first sequence contained an A-tract repeat motif that was preselected in MD simulations to reproducibly induce strong static curvature. The second sequence was "random", but with the same base pair composition. Backbone breaks were introduced at different positions to span approximately one helical turn, and the curvature was probed by PAGE. In the random fragment, single-stranded breaks produce a small retardation or virtually no effect, which agrees with earlier reports. In contrast, for the A-tract repeat nicks, a noticeable increase in the gel mobility is detected depending upon the nick position. The cumulative bending effect of the phased A-tracts and single-stranded breaks was never checked before. The positive band shifts obtained here are opposite the common nick behavior. The strongest relaxation is observed for nick positions inside A-tracts which may be due to local maxima of backbone compression. Comparison of these data with those of statically bent DNA conformations from earlier simulations suggests that this compression may result from sugar−sugar contacts in a backbone strand.

MATERIALS AND METHODS

Oligonucleotides and Construction of 5′-Labeled DNA Probes. The A-tract motif AAAATAG originally attracted our attention in MD simulations of the natural DNA fragment taken from the first curved DNA locus studied in vitro (*2*, *22*). This motif was used for constructing the 35-mer core of the A-tract repeat shown in Table 1. One of the A-tracts is inverted to make the two DNA termini symmetrical, which was essential for earlier MD simulations (*20*). To obtain a reference non-A-tract DNA, we have reshuffled manually base pairs of the A-tract repeat. We preferred this randomized sequence to commonly used GC-rich straight fragments to keep the base pair content identical and reduce the possible difference in gel mobility not related to bending. To increase the PAGE resolution of similarly bent nicked DNA, the 35-mer fragments were extended to 71 bp by adding poly(dA)·poly(dT) tails. The tails continue the mother 35-mer A-tract repeat sequence smoothly and minimize perturbations that could affect comparisons with ongoing simulations for the central part.

The double-stranded DNA containing four A-tracts flanked by poly(dA)·poly(dT) termini were constructed by annealing the two complementary synthetic oligonucleotides B^1 and B^2 (see Table 1). Double-stranded DNA fragments containing single-stranded breaks (nicks) were constructed by annealing two shorter oligonucleotides (Table 1) with the corresponding intact partner. In the same way a series of nicked duplexes was constructed from the reference random sequence fragment S, with its base pair composition identical to that of B. The design of the sequences is shown in Table 1, with nick positions shifted from the center in both directions to cover more than one helical turn. The fragment codes in this table use the following mnemonics. The capital "B" and "S" stand for "bent" and "straight". The small letter prefix "n" stands for "nick". The superscripts denote the two complementary sequences of the A-tract fragment. They are omitted when both strands are referred to simultaneously. The numbers indicate the shift of the nick position with respect to the center of the sequence.

In all the constructs, one of the oligonucleotides annealed was end-labeled with T4 polynucleotide kinase and [^{32}P]ATP. In most cases the label was attached to the 5′-end of the partner (continuous) oligonucleotide, whereas the two strands at the nick position were terminated with 3′-OH and 5′-OH

Table 1: Construction of DNA Fragments[a]

Code	Sequence
B^1	5'-A_{18}-**AAAAT**AGGCT**ATTTT**AGGCT**ATTTT**AGGCT**ATTTT**-T_{18} − 3′
nB^1+0	5'-A_{18}-**AAAAT**AGGCT**ATTTT**AG"GCT**ATTTT**AGGCT**ATTTT**-T_{18} − 3′
nB^1-2	5'-A_{18}-**AAAAT**AGGCT**ATTTT**"AGGCT**ATTTT**AGGCT**ATTTT**-T_{18} − 3′
nB^1+2	5'-A_{18}-**AAAAT**AGGCT**ATTTT**AGGC"T**ATTTT**AGGCT**ATTTT**-T_{18} − 3′
...	...
B^2	3'-T_{18}-**TTTTA**TCCGA**TAAAA**TCCGA**TAAAA**TCCGA**TAAAA**-A_{18} − 5′
B^2+0	3'-T_{18}-**TTTTA**TCCGA**TAAAA**TC"CGA**TAAAA**TCCGA**TAAAA**-A_{18} − 5′
B^2-2	3'-T_{18}-**TTTTA**TCCGA**TAAAA**"TCCGA**TAAAA**TCCGA**TAAAA**-A_{18} − 5′
B^2+2	3'-T_{18}-**TTTTA**TCCGA**TAAAA**TCCG"A**TAAAA**TCCGA**TAAAA**-A_{18} − 5′
...	...
S	5'-A_{18}-TTAGATAGTATGACTATCTATGATCATGTATGATA-T_{18} − 3′
nS+0	5'-A_{18}-TTAGATAGTATGACTAT"CTATGATCATGTATGATA-T_{18} − 3′
nS-2	5'-A_{18}-TTAGATAGTATGACT"ATCTATGATCATGTATGATA-T_{18} − 3′
nS+2	5'-A_{18}-TTAGATAGTATGACTATCT"ATGATCATGTATGATA-T_{18} − 3′
...	...

[a] A-tracts are boldfaced, and nick positions are marked by double quotes. B^1 and B^2 refer to the two complementary strands of the A-tract fragment. Nicks in the reference straight duplex S were introduced always in the same strand; therefore, the corresponding complementary sequence is not shown. In all cases shifting of the nick positions was continued from the center in both directions to cover at least one helical turn.

groups. For some sequences, 5′-phosphorylated nicks were additionally constructed to check the effect of phosphate charges. In this case the continuous strand carried 5′-OH, while ^{32}P was introduced in the corresponding shorter partner. For all constructs the oligonucleotides were gel-purified before assembly of the nicked duplexes. The annealing was carried out by incubating 300 nM unlabeled oligonucleotide(s) with 30 nM end-labeled oligonucleotide(s) for 3 min at 80 °C in 20 mM Tris−HCl (pH 8.0) and 150 mM NaCl and then allowing them to cool slowly. To distinguish between different nick series in the text, we add small letter suffixes "o" and "p" to the codes given in Table 1 for nonphosphorylated and 5′-phosphorylated nicks, respectively. Thus, the two whole nick series of the bent DNA are referred to as nB^1o and nB^1p, respectively, while the individual nicked fragments are denoted as nB^1−2o, nB^1−2p, etc.

Gel Mobility Assays. The mobility of the DNA fragments was analyzed in 12% gels (acrylamide/bisacrylamide, 29:1) buffered with 90 mM Tris−borate, pH 8.6, supplemented with 1 mM EDTA. To check the effect of Mg^{2+} ions, the Tris−borate buffer was supplemented with 10 mM $MgCl_2$ in the absence of EDTA. Gels were prerun under constant power until stabilization of the current. Labeled DNA in a buffer containing 20 mM Tris−HCl (pH 8.0), 50 mM NaCl, 4% Phicoll-400, and xylencianol was loaded onto the gel. The electrophoresis was performed under constant voltage and a constant temperature of 4 °C. The dried gels were exposed to storage phosphor screens and visualized on a Storm PhosphorImager (Molecular Dynamics).

Calculations. The results of molecular dynamics simulations used in the text are taken from our previous paper (*20*). Similar simulations of the nicked DNA fragments will be reported elsewhere.

RESULTS

Relative PAGE Mobilities. A representative PAGE plate of the random sequence series of nonphosphorylated nicks is shown in Figure 1a. All nicked DNAs exhibit similar mobilities close to that of the reference straight fragment. A weak retardation effect distinguishable for some nick positions is at the limit of experimental accuracy. Qualitatively similar patterns, but with stronger retardation, were previously reported for nicked DNA fragments under elevated temperature and/or mild denaturating conditions (*36*, *37*, *44*). We suppose, therefore, that some reduction of mobility in Figure 1a results from the isotropic flexibility at nick positions that is strongly reduced at 4 °C. This small retardation should be taken into account in the interpretation of other tests below.

The next plate, Figure 1b, compares the gel mobilities for nicks introduced in strand B^1 of the A-tract repeat. The pattern exhibited here is evidently more complex than that in Figure 1a. On one hand, for the central nick positions, the mobilities are close to that of the mother fragment, which is qualitatively similar to that of Figure 1a. However, when the nick is moved farther from the center, the PAGE mobility grows and becomes higher than that of the mother curved fragment. It reaches maximum values for nB^1−4o and nB^1+6o, but for nB^1−6o it is reduced again. As a result, the mobilities of nB^1−6o and nB^1−4o appear close to those of nB^1+4o and nB^1+6o, respectively, and the overall pattern of nick bands in Figure 1b appears skewed-sinusoidal, with the period corresponding to that of the double helix.

The same fragments with nicks introduced in the opposite strand are compared in Figure 1c. The pattern obtained is surprisingly similar to that in Figure 1b in regard to both the phases and amplitudes of the modulations. It is tempting

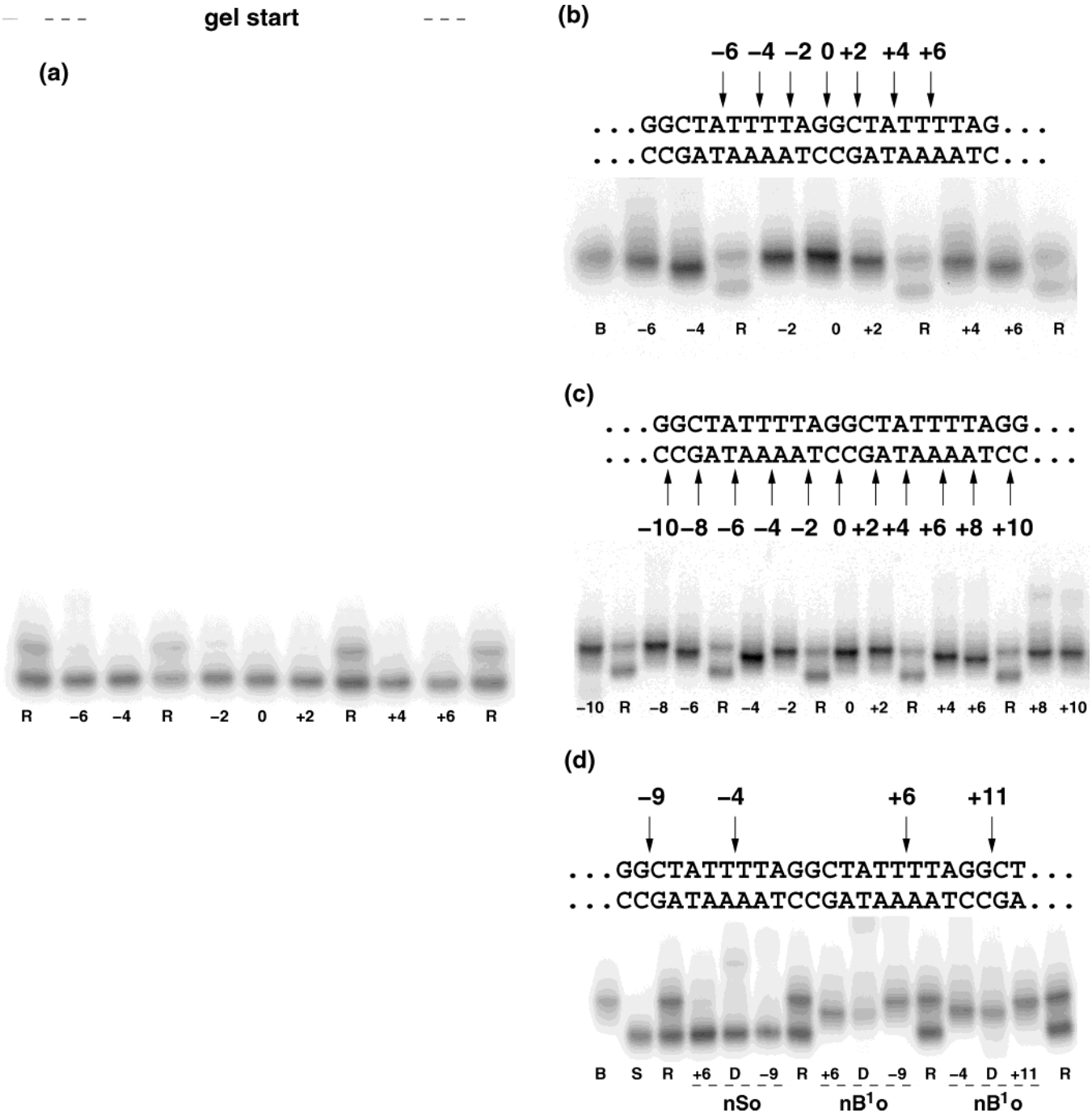

FIGURE 1: Comparison of PAGE mobilities of nicked DNA fragments. In all plates lanes "R" ("reference") contain a mixture of intact duplexes S and B. The nick positions are marked by numbers below the gel lanes. For the A-tract fragment the sequences of both strands are additionally given, with the nick positions shown by arrows. (a) Nicked random sequence fragments. Lanes "−6", ..., "+6" contain nS−6o, ..., nS+6o, respectively. (b) Nicked A-tract repeat fragments of the nB^1o series. (c) Nicked A-tract repeat fragments of the nB^2o series. (d) Double-nick fragments. Lanes marked by integer numbers contain the corresponding singly nicked DNA fragments of the series marked below the dashed lines. Lanes "D" contain fragments with the two nicks from the left and right neighbor lanes.

to assume that the local maxima of the curvature relaxation in the two strands are reached in equivalent positions with respect to the plane of the bend. In this case the bending plane should cross the central ApA steps of the A_4-tracts roughly perpendicular to their base pairs, with the corresponding nick positions facing the plane from the opposite sides. In principle, this effect can serve as another method for accurate evaluation of the local bending direction in curved DNA fragments (*45*). Other possible equivalent phosphate positions could also be considered *a priori*, namely, the intersection points of backbone strands with the bending plane and the extrema of the minor groove narrowings. In both these cases, however, the partner phosphates on the two backbones must belong to different base pair steps shifted by 3−4 residues.

The increase of PAGE mobility indicates reduced DNA curvature, and this effect can well be due to the relaxation predicted by CBH. The amplitude of the reduction is very significant since it exceeds 30% of the mobility difference between the S and B fragments due to four A-tracts. The

mobility profiles in the plates in Figure 1b,c suggest that the backbone compression is maximal within A-tracts and minimal between them. The largest positive band shifts are observed for nicks nB−4o and nB+6o that correspond to equivalent middle positions within the two consecutive A-tracts. In contrast, the effect is smaller or absent for nick positions that belong to the junction zones between A-tracts. Although this specific phasing is exactly opposite our first guess (*20*), it is accounted for by CBH. Other theories did not anticipate this effect although they can explain it *a posteriori* by introducing additional assumptions. However, there are a few simple alternative explanations that should be considered first.

The first evident factor that should be checked is the perturbed balance of phosphate charges. The two nick series displayed in Figure 1a−c have one phosphate group less than the reference fragments B and S. Consequently, their mobilities may be uniformly reduced by around 0.7%, which would mean that the apparent reduction of curvature in the nicked A-tract fragments nB−4o and nB+6o is even stronger than it is seems from Figure 1b,c. This effect, however, is not distinguishable in Figure 1a, suggesting that it is too small and may be safely neglected. The influence of phosphate charges can be more subtle, however. The electrostatic models of DNA bending assume that it is the broken balance of phosphate repulsion at the opposite DNA sides that forces it to bend (*46*). If the A-tract curvature had an electrostatic origin, the phosphate "hole" at the nick could perturb it by adding a local bend in a direction that should rotate as the hole is moved along the DNA chain. The integral curvature would be deviated and partially compensated in a way compatible with the results shown in Figure 1b,c.

To check this possibility, we prepared a series of phosphorylated nicks. Their relative PAGE mobilities are compared with other results in Figure 2. The mobility coefficients Q_m used in this plate were computed as follows. The Q_m value of the S fragment (see Table 1) is always the largest in the gel, and it is arbitrarily assumed to equal 100. The Q_m of fragment B is assumed to equal 0. For any given band its Q_m is proportional to the distance from the fastest band in the same gel (band S), and it is estimated relative to the distance between B and S. If a nicked fragment migrates slower than the B-band in the same gel, its Q_m is negative. In contrast, if it is faster, the corresponding Q_m is positive below 100. Figure 2 displays thus obtained Q_m values for all DNA fragments used in the present study.

With 5′-phosphates added to the nick sites, the phosphate holes are quenched or even inverted, which should drastically change the observed curvature modulations. The results in Figure 2, however, show the opposite. The original skewed-sinusoidal dependence is persistent. At the same time, the phosphorylated nicks exhibit uniformly reduced mobilities, which agrees with earlier reports (*36*, *37*) and should be attributed to the increased strand fraying in nicks. The additional phosphate charge increases the interstrand electrostatic repulsion at single-stranded breaks, which should enhance the fraying effect as discussed in detail elsewhere (*39*). Whatever the reason for the uniformly reduced mobility, however, these results clearly allow one to rule out the above hypothesis of electrostatic curvature compensation.

The results in Figure 1b,c can also be interpreted with the wedge model of DNA bending by assuming that nicks have

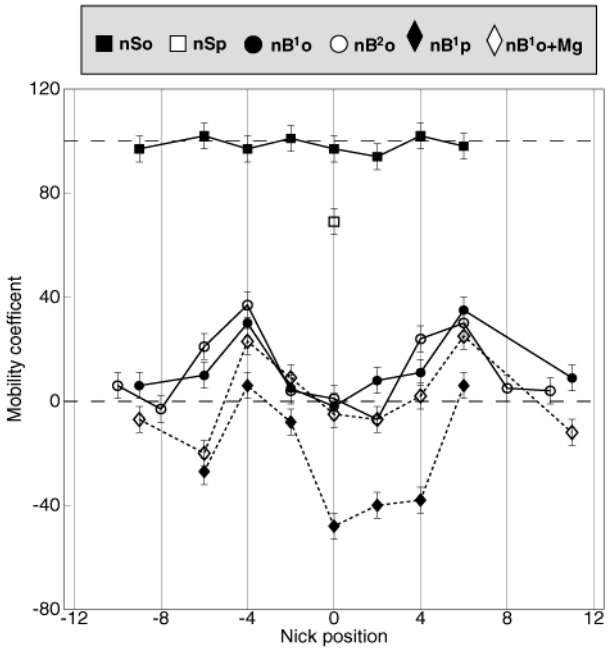

FIGURE 2: Quantitative comparison of relative mobilities of DNA fragments listed in Table 1. The method of calculation of the mobility coefficients Q_m is explained in the text. The reference mobilities of fragments B and S are indicated by horizontal dashed lines. The error bars indicate experimental errors estimated from variation of Q_m in repeated tests.

a special structure with a wedge in a fixed local direction. The overall curvature is reduced when this wedge direction is opposite that of the initial bend and increased in the opposite orientation. Similarly to the "phosphate hole" model above, sinusoidal modulations of curvature should occur as the nick site is translated along DNA. Note that this wedge should have a very large angle since it compensates in nB−4o and nB+6o more than 30% of the curvature due to four phased A-tracts. Such a strong wedge should result in an increased curvature in nB+0o as well as in the nSo series in Figure 1a, which is not seen. This interpretation also would not agree with earlier studies of nick structures and gel mobilities (*34*, *37*, *39*). However, earlier PAGE studies were carried out at higher temperatures where the isotropic flexibility of nicks could, in principle, dominate all other effects. Also, the nonlinear dependence of the gel mobility upon the curvature may be such that the acceleration effect of the nick wedge in Figure 1b is more pronounced than the expected retardation for nB+0o and the nSo series. Therefore, to check the above explanations, doubly nicked A-tract fragments were constructed, with the two sites separated by an odd number of helical half-turns so that the hypothetical wedges had opposite directions and should have compensated one another. The PAGE mobilities of doubly nicked fragments are compared in Figure 1d. These data evidently disagree with the foregoing wedge interpretation of mobility modulations. For both nB¹−4o and nB¹+6o, the addition of a second nick at 1.5 helical turn neither cancels nor even reduces the corresponding band shifts with respect to those of Figure 1b. Instead, the relaxation effects produced by two nicks appear approximately additive. As expected, analogous constructs for the random fragment S all show PAGE mobilities similar to that of the intact duplex.

Figure 2 also shows the profile of mobilities of the nB^1o series in the presence of Mg^{2+} ions. The Mg^{2+} ions are long known to affect the DNA curvature by increasing or reducing it depending upon the sequence (*47*, *48*). In our case the curvature of the A-tract repeat was increased as judged from the difference in the relative mobilities of fragments B and S, which was around 7.7% and 4.7% with and without Mg^{2+} ions, respectively. It is seen in Figure 2 that the profile of the nick mobilities in the presence of Mg^{2+} ions remains qualitatively similar, but some nicks migrated slower than the mother B fragment. Interpretation of this result depends on the assumed mechanism by which Mg^{2+} increases the A-tract curvature. If the additional bend is caused by the electrostatic attraction due to the Mg^{2+} accumulation at the inner edge of the curved DNA, the gain in the curvature may be larger when the fragment is nicked, and this effect would compete with the curvature relaxation. Other explanations are also possible. Multivalent cations should push other similar charges from their environment, and their distribution around DNA is probably more stable and structure specific. This should influence the screening of phosphate charges, with possibly different effects for short- and long-range interactions. If the local screening is reduced at nicks due to specific ion positioning, the increased strand fraying may produce negative Q_m values in the same way as for the phosphorylated nicks. In any case, this effect of Mg^{2+} upon the curvature modulations evidences that there is an intricate relationship between the electrostatic DNA environment and its structure. However, the curvature relaxation remains persistent, suggesting that it is not directly related to the strong interactions between DNA charges as well as their counterion environment.

Possible Source of Backbone Compression. The experimental results presented above evidence that single-stranded breaks relax the overall curvature of the A-tract repeat in remarkable qualitative agreement with CBH. They suggest that the backbone compression should increase inside A-tracts and reduce outside them. Because A-tracts are found at the inner edge of the curved double helix, the last suggestion agrees with the simple intuition that says that the surface of a curved cylinder is compressed at its inner edge and stretched at the opposite side. To guess which backbone component may be responsible for the compression, we tried to measure variation of the backbone density in strongly bent computed structures obtained in long-time molecular dynamics simulations reported earlier (*20*).

The local backbone length/density is usually characterized by intra-phosphate distances (*49*), but we decided to check other atoms as well. It appeared that, regardless of the reference atoms chosen, the computed density profiles are very noisy and regular modulations can be seen only after averaging with a sliding window. Nevertheless, it was readily found that different interatom distances exhibited qualitatively different patterns and that all backbone atoms can be divided into two groups. For phosphates and their neighbors, the interatom distances are usually larger at the inner side of the bend and smaller at the opposite side, which may be viewed as a trend toward the A-form in the widenings of the major groove. These modulations are very small, in agreement with the conventional view of the B-DNA backbone as being noncompressible (*49*). The second group involves O4′ atoms and their neighbors. In this case, modulations are stronger and their phases are opposite those in the first group; that is, they exhibit an increase of backbone density at the inner side of the bend. It should be noted that two qualitatively similar groups of backbone atoms are distinguished in X-ray structures of bent DNA (*50*) (A.K.M., unpublished results). The CBH does not specify which atom−atom interactions cause the backbone compression; however, the gel mobility data reported here suggest that the second of the aforementioned two groups can be involved in this effect.

The backbone density profiles produced by O4′ atoms are shown in Figure 3. The data were accumulated during the last 8 ns of a 12 ns trajectory that started from canonical B-DNA and, after 4 ns, converged to a stable strong bend toward the narrowed minor grooves of the A-tracts (*20*). For better comparison with experiments, the profiles were computed separately for strands B^1 and B^2 as well as for both of them together. The amplitudes of smooth modulations attributed to the bent DNA shape are well beyond dynamic fluctuations. The two strands look rather dissimilar, with the B^2 plots more regular than those of B^1, and the two strands making asymmetrical contributions to the average backbone length, which is attributed to their rather different sequences. In Figure 2, the difference between strands B^1 and B^2 looks less significant. Also, the orientation of the best fit bending plane marked by vertical bars in Figure 3 somewhat differs from that estimated from the experiments above. At the same time, the backbone length reaches clear local minima at the inner edge of the bend close to the centers of the A_4-tracts where maximal curvature relaxation is observed.

These results demonstrate that the DNA backbone behaves as a complex mechanical system rather than a chain of strings or rigid rods, and that its different components compress and stretch in different zones of the curved DNA. Definite conclusions concerning the possible relationship between the oscillations observed in Figures 2 and 3 are premature. Additional experiments and simulations with other A-tract sequences are necessary to study these effects in more detail and establish precisely which atom−atom interactions may cause the backbone compression and relaxation. Nevertheless, the correlations revealed in Figure 3 prove that certain backbone components behave in curved DNA as predicted by CBH and suggest that the backbone compression, if it really exists, may result from sugar−sugar interactions. Even though in B-DNA consecutive O4′ atoms do not interact, the neighboring sugar rings make a number of direct contacts nonmediated by the solvent.

DISCUSSION AND CONCLUSIONS

The present experimental investigation reveals previously unknown features in the intrinsic DNA curvature that may shed new light upon its putative mechanism. This intriguing phenomenon seems to be exhaustively studied, but it still attracts great interest. Already in the 1970s, it was realized that the DNA double helix is not a rigid cylinder, but is bendable depending upon the direction and the base pair sequence (*51*, *52*). By postulating that stacking in ApA steps is intrinsically nonparallel, the wedge model predicted that A-tracts repeated in phase with the helical screw should bend DNA (*53*). This proved true, but the model later appeared unsatisfactory. It turned out that X-ray DNA structures are

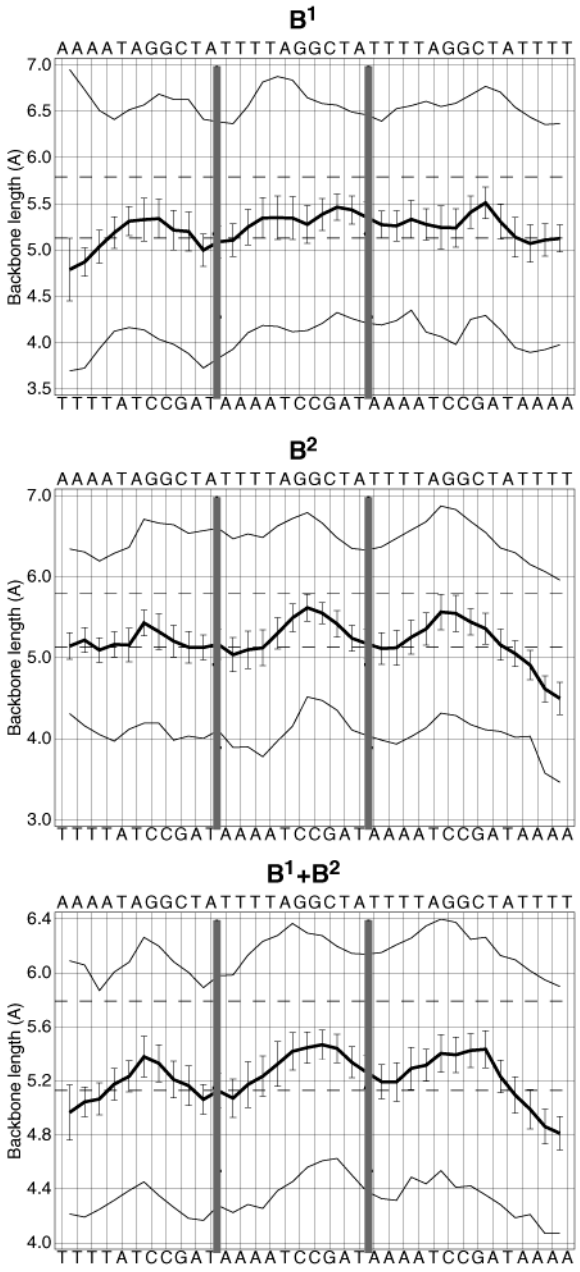

FIGURE 3: Backbone length profile averaged over 8 ns of a molecular dynamics trajectory of fragment B. The plots were obtained as explained in the text. The three plates refer to strands B^1, B^2, and their average. The corresponding sequences are given at the top and bottom of all plates for B^1 and B^2, respectively. The central traces in all plates show the local length averaged over the whole period with rms fluctuations shown as error bars. The upper and lower solid traces show the maximal and minimal values, respectively. All profiles were smoothed with a sliding window of three base pair steps. The length is given in angströms, with the corresponding canonical A- and B-DNA levels indicated by the horizontal dashed lines. The vertical gray bars mark the approximate orientation of the computed optimal bending plane that passed nearly perpendicular to the AT base pairs at the 3′-ends of the A_4-tracts (*20*).

often bent in random sequences whereas A-tracts are exceptionally straight (*54*−*56*). With the growing number of sequences checked, nonzero wedges had to be introduced for all base pair steps (*5*, *6*); nevertheless, experimental counterexamples were eventually found where bending could not result from accumulation of wedges (*57*, *58*). Several theories tried to reveal other factors involved in DNA bending along with local stacking interactions. The junction model proposed by Crother's group (*59*, *2*) originated from an idea that a bend should occur when two different DNA forms are stacked (*60*). If the poly(dA)·poly(dT) double helix had a special B′ form as suggested by some data (*61*), the helical axis should be kinked when an A-tract is interrupted by a random sequence. Drew and Travers (*25*, *26*) apparently were the first to notice that narrowing of both DNA grooves at the inner edge of a bend is a necessary and sufficient condition of bending. They, and later Burkhoff and Tullius (*27*), considered the preference of narrow and wide minor groove profiles by certain sequences as the possible original cause of this effect. In recent years, the idea of an electrostatic origin of curvature gained strong support, with various roles attributed to solvent counterions (*62*−*67*). Detailed analyses of all these theories can be found in the recent literature (*11*, *12*, *20*). Each of the aforementioned mechanisms is supported by specific experimental data. Probably they all correctly describe different aspects of this complex phenomenon, although none of them are able to relieve all the controversies and account for the growing number of perplexing results (*13*, *68*).

Both the A-tract repeats and single-stranded breaks have been previously recognized as elements specifically involved in DNA bending. To our best knowledge, however, nobody checked what could be their cumulative effect. Here it is found that nicks relax the intrinsic curvature induced by A-tract repeats in conditions where they do not affect the random sequence DNA. The relaxation effect depends on the nick position with respect to the bend, and as shown here, it cannot be attributed to new wedges due to local perturbations or electrostatic effects. It is very significant when the nick is at the inner edge of the bent DNA inside A-tracts, and is gradually reduced essentially to zero when the nick is moved to the outer surface of the bend. This behavior is in qualitative agreement with the CBH, and it suggests that the backbone compression in the curved DNA is larger in the minor groove narrowings at the inner surface. Inspection of the DNA conformations obtained in earlier molecular dynamics simulations reveals strong regular modulations of the local backbone length as measured by distances between certain sugar atoms, with compression reaching its maximum at the inner edge of the bend where nicks produce the strongest relaxation in experiments. These results provide additional support to the CBH and suggest that the frustration in the B-DNA backbone may result from interactions between consecutive sugar rings. They also confirm involvement in DNA bending of other factors such as free Mg^{2+} ions.

The first idea of our experiments came from the CBH, and the present investigation was intended to distinguish it from prevailing theories of DNA bending that could not anticipate these results. However, the last consideration does not necessarily mean that these alternative theories are disproved. Other interpretations of our data should also be considered. For instance, in the context of the junction theory, one can postulate that single-stranded breaks perturb the specific B′ structure of A-tracts in a specific position-dependent manner corresponding to the curvature relaxation profiles in Figure 1. A similar interpretation can be formulated for the modified wedge model that includes several base pair steps in a wedge. These would be strong assump-

tions, however, because, on one hand, these perturbations should produce a significant effect upon the gel mobilities but, on the other hand, they are not visible in the X-ray structure of a nicked A-tract (*34*). Future experiments with curved non-A-tract DNA fragments may help to check if the curvature relaxation is specific to A-tracts. To explain our data with the counterion models, one should assume that nicks specifically affect the counterion shells. An exhaustive discussion of all possible interpretations is beyond our present purposes. Additional studies are certainly necessary to establish precisely the origin of the curvature relaxation revealed here. The DNA bending is a complex phenomenon that has many faces, with different mechanisms discussed in the literature playing their roles together. The backbone compression, which we believe really exists, is an essential element that was missing in previous studies and that can shed new light upon many earlier observations in this field.

REFERENCES

1. Marini, J. C., Levene, S. D., Crothers, D. M., and Englund, P. T. (1982) Bent helical structure in kinetoplast DNA, *Proc. Natl. Acad. Sci. U.S.A. 79*, 7664−7668.
2. Wu, H.-M., and Crothers, D. M. (1984) The locus of sequence-directed and protein-induced DNA bending, *Nature 308*, 509−513.
3. Hagerman, P. J. (1984) Evidence for the existence of stable curvature of DNA in solution, *Proc. Natl. Acad. Sci. U.S.A. 81*, 4632−4636.
4. Griffith, J., Bleyman, M., Rauch, C. A., Kitchin, P. A., and Englund, P. T. (1986) Visulatization of the bent helix in kinetoplast DNA by electron microscopy, *Cell 46*, 717−724.
5. Bolshoy, A., McNamara, P., Harrington, R. E., and Trifonov, E. N. (1991) Curved DNA without A-A. Experimental estimation of all 16 DNA wedge angles, *Proc. Natl. Acad. Sci. U.S.A. 88*, 2312−2316.
6. McNamara, P. T., and Harrington, R. E. (1991) Characterization of inherent curvature in DNA lacking polyadenine runs, *J. Biol. Chem. 266*, 12548−12554.
7. Diekmann, S. (1987) DNA curvature, in *Nucleic Acids and Molecular Biology* (Eckstein, F., and Lilley, D. M. J., Eds.) Vol. 1, pp 138−156, Springer-Verlag, Berlin.
8. Hagerman, P. J. (1990) Sequence-directed curvature of DNA, *Annu. Rev. Biochem. 59*, 755−781.
9. Crothers, D. M., Haran, T. E., and Nadeau, J. G. (1990) Intrinsically bent DNA, *J. Biol. Chem. 265*, 7093−7096.
10. Crothers, D. M., and Drak, J. (1992) Global features of DNA structure by comparative gel electrophoresis, *Methods Enzymol. 212*, 46−71.
11. Olson, W. K., and Zhurkin, V. B. (1996) Twenty years of DNA bending, in *Structure and Dynamics. Vol. 2: Proceedings of the Ninth Conversation, State University of New York, Albany, N.Y. 1995* (Sarma, R. H., and Sarma, M. H., Eds.) pp 341−370, Adenine Press, New York.
12. Crothers, D. M., and Shakked, Z. (1999) DNA bending by adenine-thymine tracts, in *Oxford Handbook of Nucleic Acid Structure* (Neidle, S., Ed.) pp 455−470, Oxford University Press, New York.
13. Merling, A., Sagaydakova, N., and Haran, T. E. (2003) A-tract polarity dominate the curvature in flanking sequences, *Biochemistry 42*, 4978−4984.
14. Jerkovic, B., and Bolton, P. H. (2000) The curvature of dA tracts is temperature dependent, *Biochemistry 39*, 12121−12127.
15. Jerkovic, B., and Bolton, P. H. (2001) Magnesium increases the curvature of duplex DNA that contains dA tracts, *Biochemistry 40*, 9406−9411.
16. MacDonald, D., Herbert, K., Zhang, X., Polgruto, T., and Lu, P. (2001) Solution structure of an A-tract DNA bend, *J. Mol. Biol. 306*, 1081−1098.
17. Hizver, J., Rozenberg, H., Frolow, F., Rabinovich, D., and Shakked, Z. (2001) DNA bending by an adenine-thymine tract and its role in gene regulation, *Proc. Natl. Acad. Sci. U.S.A. 98*, 8490−8495.
18. Hud, N. V., and Feigon, J. (2002) Characterization of divalent cation localization in the minor groove of the A(n)T(n) and T(n)A(n) DNA sequence elements by (1)H NMR spectroscopy and manganese(II), *Biochemistry 41*, 9900−9910.
19. Møllegaard, N. E., and Nielsen, P. I. (2003) Increased temperature and 2-methyl-2,4-pentanediol change the DNA structure of both curved and uncurved adenine/thymine-rich sequences, *Biochemistry 42*, 8587−8593.
20. Mazur, A. K., and Kamashev, D. E. (2002) Simulated and experimental bending dynamics in DNA with and without regularly repeated adenine tracts, *Phys. Rev. E 66*, 011917(1−13).
21. Mazur, A. K. (2000) Theoretical studies of the possible origin of intrinsic static bends in double helical DNA, *J. Am. Chem. Soc. 122*, 12778−12785.
22. Mazur, A. K. (2001) Molecular dynamics studies of sequence-directed curvature in bending locus of Trypanosome kinetoplast DNA, *J. Biomol. Struct. Dyn. 18*, 832−843.
23. Watson, J. D., and Crick, F. H. C. (1953) A structure for deoxyribose nucleic acid, *Nature 171*, 737−738.
24. Ediger, M. D. (2000) Spatially heterogeneous dynamics in supercooled liquids, *Annu. Rev. Phys. Chem. 51*, 99−128.
25. Drew, H. R., and Travers, A. A. (1984) DNA structural variations in the E.coli tyrT promoter, *Cell 37*, 491−502.
26. Drew, H. R., and Travers, A. A. (1985) DNA bending and its relation to nucleosome positioning, *J. Mol. Biol. 186*, 773−790.
27. Burkhoff, A. M., and Tullius, T. D. (1987) The unusual conformation adopted by the adenine tracts in kinetoplast DNA, *Cell 48*, 935−943.
28. Thomas, C. A., Jr. (1956) The enzymatic degradation of deoxyribose nucleic acid, *J. Am. Chem. Soc. 78*, 1861−1868.
29. Hays, J. B., and Zimm, B. H. (1970) Flexibility and stiffness in nicked DNA, *J. Mol. Biol. 48*, 297−317.
30. Shore, D., and Baldwin, R. L. (1983) Energetics of DNA twisting, *J. Mol. Biol. 170*, 957−981.
31. Hsieh, C. H., and Griffith, J. D. (1989) Deletions of bases in one strand of duplex DNA, in contrast to single-base mismatches, produce highly kinked molecules: Possible relevance to the folding of single-stranded nucleic acids, *Proc. Natl. Acad. Sci. U.S.A. 86*, 4833−4837.
32. Pieters, J. M. L., Mans, R. M. W., van den Elst, H., van der Marel, G. A., van Boom, J. H., and Altona, C. (1989) Conformational and thermodynamics consequences of the introduction of a nick in duplex DNA fragments: An NMR study augmented by biochemical experiments, *Nucleic Acids Res. 17*, 4551−4565.
33. Snowden-Ifft, E. A., and Wemmer, D. E. (1990) Characterization of the structure and melting of DNAs containing backbone nicks and gaps, *Biochemistry 29*, 6017−6025.
34. Aymami, J., Coll, M., van der Marel, G. A., van Boom, J. H., Wang, A. H.-J., and Rich, A. (1990) Molecular structure of nicked DNA: A substrate for DNA repair enzymes, *Proc. Natl. Acad. Sci. U.S.A. 87*, 2526−2530.
35. Rentzeperis, D., Ho, J., and Marky, L. A. (1993) Contribution of loops and nicks to the formation of DNA dumbbells: Melting behavior and ligand binding, *Biochemistry 29*, 2564−2572.
36. Le Cam, E., Fack, F., Ménissier-de Murcia, J., Cognet, J. A. H., Barbin, A., Sarantoglou, V., Révet, B., Delain, E., and de Murcia, G. (1994) Conformational analysis of a 130 base-pair DNA fragment containing a single-stranded break and its interaction with human poly(ADP-ribose) polymerase, *J. Mol. Biol. 235*, 1062−1071.
37. Mills, J. B., Kooper, J. P., and Hagerman, P. J. (1994) Electrophoretic evidence that single-stranded regions of one or more nucleotides dramatically increase the flexibility of DNA, *Biochemistry 33*, 1797−1803.
38. Hagerman, K. R., and Hagerman, P. J. (1996) Helix rigidity of DNA: The meroduplex as an experimental paradigm, *J. Mol. Biol. 260*, 207−223.
39. Furrer, P., Bednar, J., Stasiak, A. Z., Katritch, V., Michoud, D., Stasiak, A., and Dubochet, J. (1997) Opposite effect of counterions on the persistence length of nicked and non-nicked DNA, *J. Mol. Biol. 266*, 711−721.
40. Lane, M. J., Paner, T., Kashin, I., Faldasz, B. D., Li, B., Gallo, F. J., and Benight, A. S. (1997) The thermodynamics advantage of DNA oligonucleotide 'stacking hybridization' reactions: Energetics of a DNA nick, *Nucleic Acids Res. 25*, 611−617.
41. Singh, S., Patel, P. K., and Hosur, R. H. (1997) Structural polymorphism and dynamism in the DNA segment GATCTTC-CCCCCGGAA: NMR investigations of hairpin, dumbbell, nicked duplex, parallel strands, and i-motif, *Biochemistry 36*, 13214−13222.

42. Roll, C., Ketterlé, C., Faibis, V., Fazakerley, G. V., and Boulard, Y. (1998) Conformations of nicked and gapped DNA structures by NMR and molecular dynamic simulations in water, *Biochemistry 37*, 4059−4070.
43. Kozerski, L., Mazurek, A. B., Kawecki, R., Bocian, W., Krajewski, P., Bednarek, E., Sitkowski, J., Williamson, M. P., Moir, A. J. G., and Hansen, P. E. (2001) A nicked duplex decamer DNA with a PEG6 tether, *Nucleic Acids Res. 29*, 1132−1143.
44. Kuhn, H., Protozanova, E., and Demidov, V. V. (2002) Monitoring of single nicks in duplex DNA by gel electrophoretic mobility-shift assay, *Electrophoresis 23*, 2384−2387.
45. Zinkel, S. S., and Crothers, D. M. (1987) DNA bend direction by phase sensitive detection, *Nature 328*, 178−181.
46. Hud, N. V., and Polak, M. (2001) DNA-cation interactions: The major and minor grooves are flexible ionophores, *Curr. Opin. Struct. Biol. 11*, 293−301.
47. Diekmann, S., and Wang, J. C. (1985) On the sequence determinants and flexibility of the kinetoplast DNA fragment with abnormal gel electrophoretic mobilities, *J. Mol. Biol. 186*, 1−11.
48. Diekmann, S. (1987) Temperature and salt dependence of gel migration anomaly of curved DNA fragments, *Nucleic Acids Res. 15*, 247−265.
49. Calladine, C. R., and Drew, H. R. (1992) *Understanding DNA: The molecule & how it works*, Academic Press, London.
50. Richmond, T. J., and Davey, C. A. (2003) The structure of DNA in the nucleosome core, *Nature 423*, 145−150.
51. Namoradze, N. Z., Goryunov, A. N., and Birshtein, T. M. (1977) On conformations of the superhelix structure, *Biophys. Chem. 7*, 59−70.
52. Zhurkin, V. B., Lysov, Y. P., and Ivanov, V. I. (1979) Anisotropic flexibility of DNA and the nucleosomal structure, *Nucleic Acids Res. 6*, 1081−1096.
53. Trifonov, E. N., and Sussman, J. L. (1980) The pitch of chromatin DNA is reflected in its nucleotide sequence, *Proc. Natl. Acad. Sci. U.S.A. 77*, 3816−3820.
54. Calladine, C. R., Drew, H. R., and McCall, M. J. (1988) The intrinsic curvature of DNA in solution, *J. Mol. Biol. 201*, 127−137.
55. Maroun, R. C., and Olson, W. K. (1988) Base sequence effects in double-helical DNA. III. Average properties of curved DNA, *Biopolymers 27*, 585−603.
56. Dickerson, R. E., Goodsell, D. S., and Neidle, S. (1994) '... the tyranny of the lattice ...', *Proc. Natl. Acad. Sci. U.S.A. 91*, 3579−3583.
57. Dlakic, M., and Harrington, R. E. (1996) The effects of sequence context on DNA curvature, *Proc. Natl. Acad. Sci. U.S.A. 93*, 3847−3852.
58. Dlakic, M., and Harrington, R. E. (1998) Unconventional helical phasing of repetitive DNA motifs reveals their relative bending contributions, *Nucleic Acids Res. 26*, 4274−4279.
59. Levene, S. D., and Crothers, D. M. (1983) A computer graphics study of sequence-directed bending of DNA, *J. Biomol. Struct. Dyn. 1*, 429−435.
60. Selsing, E., Wells, R. D., Alden, C. J., and Arnott, S. (1979) Bent DNA: Visualization of a base-paired and stacked A-B conformational junctions, *J. Biol. Chem. 254*, 5417−5422.
61. Alexeev, D. G., Lipanov, A. A., and Skuratovskii, I. Y. (1987) Poly(dA).poly(dT) is a B-type double helix with a distingtively narrow minor groove, *Nature 325*, 821−823.
62. Levene, S. D., Wu, H.-M., and Crothers, D. M. (1986) Bending and flexibility of kinetoplast DNA, *Biochemistry 25*, 3988−3995.
63. Young, M. A., Jayaram, B., and Beveridge, D. L. (1997) Intrusion of counterions into the spine of hydration in the minor groove of B-DNA: Fractional occupancy of electronegative pockets, *J. Am. Chem. Soc. 119*, 59−69.
64. Rouzina, I., and Bloomfield, V. A. (1998) DNA bending by small, mobile multivalent cations, *Biophys. J. 74*, 3152−3164.
65. Strauss, J. K., and Maher, L. J., III (1994) DNA bending by asymmetric phosphate neutralization, *Science 266*, 1829−1834.
66. Williams, L. D., and Maher, L. J., III (2000) Electrostatic mechanisms of DNA deformation, *Annu. Rev. Biophys. Biomol. Struct. 29*, 497−521.
67. Hud, N. V., and Plavec, J. (2003) A unified model for the origin of DNA sequence-directed curvature, *Biopolymers 69*, 144−159.
68. Dlakic, M., Park, K., Griffith, J. D., Harvey, S. C., and Harrington, R. E. (1996) The organic crystallizing agent 2-methyl-2,4-pentanediol reduces DNA curvature by means of structural changes in A-tracts, *J. Biol. Chem. 271*, 17911−17919.

BI036266A